Anti-cancer potency and structural insights of synthesized metformin–phenolic acid hybrids through molecular docking and dynamics simulations

Biswajit Banerjee[1], Tripti Sharma[1,2], and Arijit Mondal[3]*

ABSTRACT

Cancer remains a major global cause of death, driving the continuous search for innovative and effective treatments. In this context, we synthesized a series of 10 new hybrid compounds (M1–M10) by combining metformin (MET), a widely used anti-diabetic drug with emerging anti-cancer properties, and 10 different phenolic acids (A1–A10), known for their antioxidant and anti-cancer effects. To investigate their potential, we selected two target enzymes implicated in cancer progression—arachidonate 5-lipoxygenase (Protein Data Bank ID: 7TTL) and matrix metalloproteinase 9 (MMP9; PDB ID: 1GKC)—for molecular docking using AutoDock 4.2. Based on drug-likeness predictions and docking results, we further performed 100-nanosecond molecular dynamics simulations in GROMACS 2022 on four complexes—MMP9–A3, MMP9–M3, MMP9–MET, and MMP9–marimastat—to assess their stability and interactions at the atomic level. In comparison with individual phenolic acids (–6 to –8 kcal/mol), MET (–6 to –8 kcal/mol), and the reference inhibitor marimastat (–5 kcal/mol), the synthesized hybrids showed greater binding affinities, ranging from –7 to –10 kcal/mol, according to molecular docking studies. Molecular dynamics simulations, evaluated through parameters, such as root-mean-square deviation, root-mean-square fluctuation, radius of gyration, and hydrogen bond interaction profiles, demonstrated that the MMP9–M3 complex showed superior stability, higher drug-likeness, and lower predicted toxicity compared with the other studied complexes. Overall, the results indicate that the synthesized hybrids, especially M3, are the most promising candidates in the series. In conclusion, the design of hybrid compounds appears to be a practical approach for discovering novel phytochemical-based anti-cancer agents. In addition, the use of bioinformatics tools is crucial for streamlining the identification of the most promising lead compounds and optimizing experimental outcomes.

Keywords:
Anti-cancer hybrid agents; Metformin; Phenolic acids; Molecular docking and dynamic simulation; Drug-likeness profile

***Corresponding author:**
Arijit Mondal,
juarijitmondal@gmail.com

How to cite this article:
Banerjee, B.; Sharma, T.; Mondal, A. Anti-cancer potency and structural insights of synthesized metformin–phenolic acid hybrids through molecular docking and dynamics simulations. *Biomater Transl.* 2026, 7(3), 435-445.

doi: 10.12336/bmt.25.00038

1. Introduction

Cancer continues to pose a significant global public health challenge, with persistently high prevalence and mortality rates. At present, the second leading cause of death worldwide, cancer, is associated with increasing numbers of new cases and fatalities. By 2040, annual cancer cases are estimated to rise to 29.5 million, accompanied by 16.4 million deaths.[1-4] Despite advances in diagnostic and therapeutic methods, the side effects of present treatments and the complex, heterogeneous nature of cancer subtypes perpetuate disparities in outcomes.[5,6] Significant progress in understanding the molecular basis of cancer has enabled the identification of critical targets involved in tumor growth, survival, and metastasis.[6-8] This knowledge has fueled

the development of targeted anti-cancer agents designed to improve efficacy while minimizing toxicity. Although these approaches offer advantages, challenges, such as drug resistance, tumor heterogeneity, and the limited reliability of pre-clinical models remain. These challenges underscore the urgent need for more reliable and physiologically relevant drug screening platforms to accelerate the development of safer and more effective anti-cancer therapies.

There has been growing interest in plant-derived secondary metabolites, also known as phytochemicals, in the search for low-toxicity, cost-effective potential anti-cancer regimens.[9-11] Phytochemicals comprise a broad and diverse group of bioactive compounds that can influence various cellular processes involved in cancer initiation and progression.[10,11] Their structural diversity includes classes, such as alkaloids, flavonoids, and terpenoids, as well as unique molecular frameworks, such as indole, imidazole, benzofuran, and naphthoquinones.[12-14] Importantly, these compounds generally exhibit low toxicity toward normal cells. Phenolic acids, encompassing benzoic and cinnamic acid derivatives, are a notable subset of phytochemicals found in many plant-based foods and beverages, known for their wide-ranging biological activities and potential roles in cancer prevention and treatment. Numerous studies highlight their capacity to interfere with cancer cell functions by disrupting microtubule dynamics and triggering apoptosis. Nevertheless, challenges related to their bioavailability, optimal dosing, target specificity, and successful clinical translation must be addressed to fully realize their therapeutic potential.[15] Consequently, innovative and scientifically rigorous drug screening strategies capable of accurately evaluating the therapeutic potential of phytochemicals are essential for advancing next-generation anti-cancer therapies.

Researchers are increasingly combining active phytochemicals with existing drugs to create hybrid formulations, presenting a promising approach to drug discovery and addressing limited treatment options.[16-19] The literature reveals the potential to repurpose established drugs to treat multiple diseases by targeting a single enzyme. Metformin (MET), a commonly prescribed anti-diabetic medication, has garnered attention due to its potential anti-cancer properties, which have been explored through structural optimization, chemical modification, hybridization, and synergistic formulation.[20-22] MET is highly water-soluble and lowers glucose levels by modulating cellular energy metabolism rather than acting as a target-specific inhibitor. Its anti-cancer effects are mediated by multiple mechanisms, including the activation of AMP-activated protein kinase and the regulation of insulin signaling pathways.[21,23-25] Structural alterations and the combination of MET with other pharmacophores can potentially enhance its efficacy against cancer while overcoming challenges, such as low bioavailability and side effects. Advances in medicinal chemistry have led to the development of various MET derivatives and hybrids with enhanced pharmacokinetic and pharmacodynamic profiles, exhibiting promising anti-cancer activity through diverse mechanisms.[26,27]

Our previous paper reported the synthesis and characterization of 10 hybrid candidates (M1–M10) that combine MET with different phenolic acids.[28] These compounds demonstrated promising therapeutic potential for cancer treatment. In this study, we employed a computer-aided drug design platform to evaluate the anti-cancer efficacy, toxicity profiles, structural characteristics, and drug-likeness properties of these compounds. This comprehensive computational approach aims to identify the most promising hybrid candidate for subsequent experimental validation, thereby enhancing the likelihood of success in clinical trials.

A systematic literature search was conducted across PubMed, Scopus, Web of Science, and Google Scholar through June 2025 to identify studies on MET–phenolic acid hybrids and their anti-cancer potential. The search used combinations of keywords, such as "metformin–phenolic acid hybrids," "ALOX5 inhibition," "MMP-9 inhibition," "molecular docking," and "molecular dynamics simulation." Relevant peer-reviewed articles and computational studies were included, while non-English publications, incomplete reports, and unrelated studies were excluded. The selected references provided a comprehensive foundation for the design, docking, and molecular dynamics analyses conducted in this study.

2. Materials and methods

The *in silico* study was performed on the Linux-Ubuntu 20.04 (Canonical Ltd, England) operating system, utilizing a range of bioinformatics and cheminformatics software tools to systematically conduct the computational analyses.[29,30] All chemical structures and schematic illustrations were created using ChemDraw Professional (v20.0; PerkinElmer, United States of America [USA]) and BioRender (BioRender.com, Canada), respectively. These software tools were employed to ensure high-quality, original images suitable for publication. No copyrighted or previously published material from third parties was used in preparing the figures for this study.

2.1. Computational protocols for ligand setup and target selection in molecular docking

We selected 10 phenolic acids—benzoic acid (A1), cinnamic acid (A2), caffeic acid (A3), ferulic acid (A4), gallic acid (A5), *para*-hydroxybenzoic acid (A6), *para*-coumaric acid (A7), protocatechuic acid (A8), salicylic acid (A9), and vanillic acid (A10)—from the literature to synthesize 10 MET–phenolic acid derivatives: MET–benzoic acid conjugate $C_{11}H_{15}N_5O$ (M1), MET–cinnamic acid conjugate $C_{13}H_{17}N_5O$ (M2), MET–caffeic acid conjugate $C_{13}H_{17}N_5O_3$ (M3), MET–ferulic acid conjugate $C_{14}H_{19}N_5O_3$ (M4), MET–gallic acid conjugate $C_{11}H_{15}N_5O_4$

[1]Department of Pharmaceutical Chemistry, School of Pharmaceutical Sciences, Siksha "O" Anusandhan, Bhubaneswar, Odisha, India; [2]Department of Pharmaceutical Chemistry, Bombay College of Pharmacy, Mumbai, Maharashtra, India; [3]Department of Pharmaceutical Chemistry, Anand College of Education, Paschim Medinipur, West Bengal, India

(M5), MET–*para*-hydroxybenzoic acid conjugate $C_{11}H_{15}N_5O_2$ (M6), and MET–coumaric acid conjugate $C_{13}H_{17}N_5O_2$ (M7), MET–protocatechuic acid conjugate $C_{11}H_{15}N_5O_3$ (M8), MET–salicylic acid conjugate $C_{11}H_{15}N_5O_2$ (M9), and MET–vanillic acid conjugate $C_{12}H_{17}N_5O_3$ (M10).[28] **Figure 1** illustrates the synthetic pathway and chemical structures of the synthesized hybrids. The hybrid compounds were drawn using ChemDraw 20.0 (PerkinElmer, USA) and saved as individual.mol files.[31,32] The native phytochemical MET and two standard anti-cancer drugs were retrieved from the PubChem data archive in a structure data file (.sdf) format. Native, hybrid, and standard drug structures were then optimized in Avogadro (an open-source molecular builder and visualization tool; http://avogadro.cc/) and subsequently used as ligands in virtual screening and molecular docking studies. The Swiss Target Prediction tool (https://www.swisstargetprediction.ch) and a literature review were employed to identify two cancer-associated enzymes, arachidonate 5-lipoxygenase (ALOX5) and matrix metalloproteinase 9 (MMP-9), as potential targets. Their crystallographic structures were retrieved from the Protein Data Bank (PDB IDs: 7TTL for ALOX5 and 1GKC for MMP9), and molecular docking studies were performed. Doxorubicin (DOX) and marimastat (MT or BB-2516) were used as standard drugs for comparison.[32] Virtual screening and

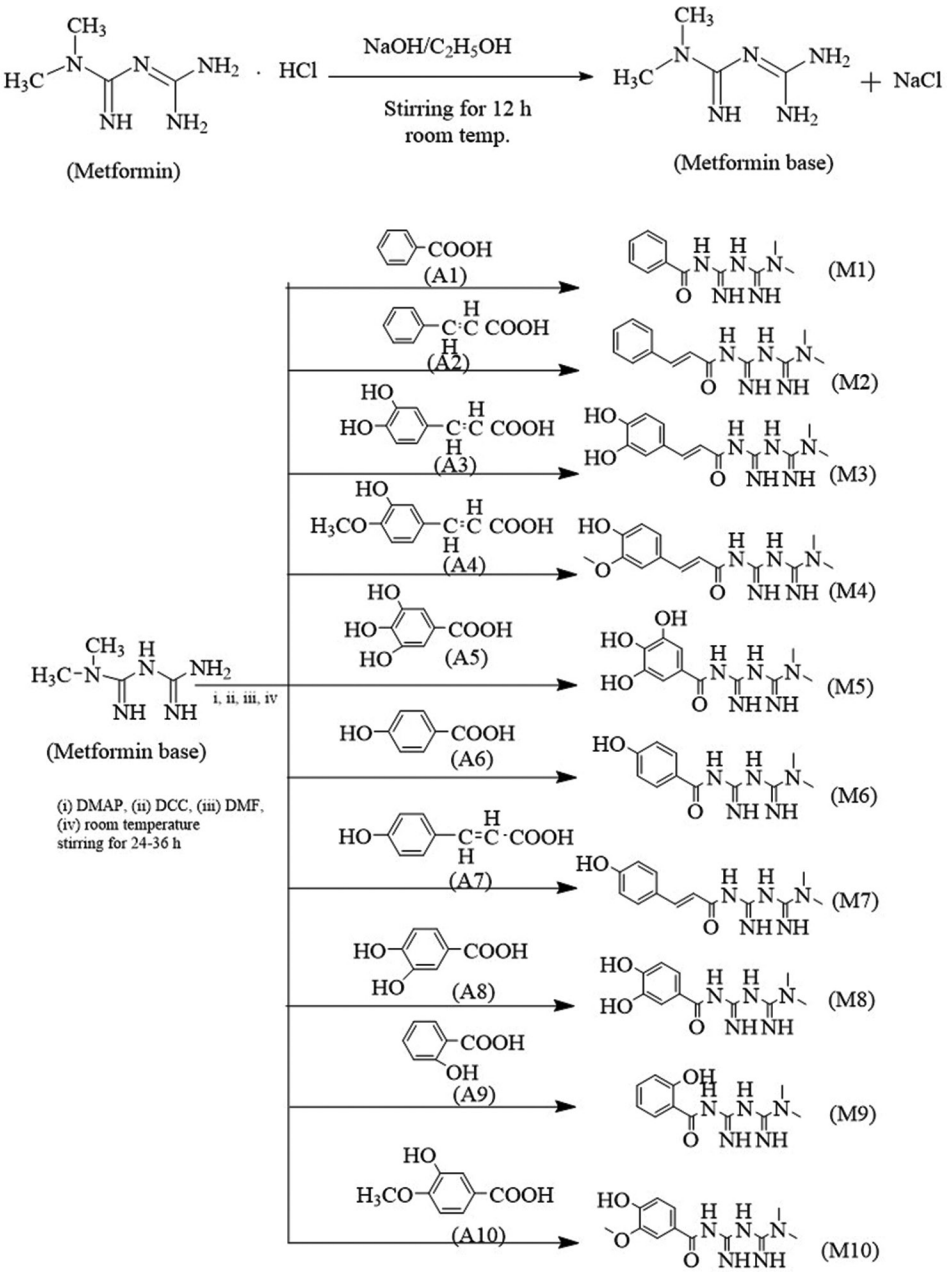

Figure 1. Synthetic pathway and chemical structures of the synthesized hybrids

Abbreviations: DCC: Dicyclohexylcarbodiimide; DMAP: 4-dimethylaminopyridine; DMF: Dimethylformamide; M1: Metformin (MET)–benzoic acid conjugate; M2: MET–cinnamic acid conjugate; M3: MET–caffeic acid conjugate; M4: MET–ferulic acid conjugate; M5: MET–gallic acid conjugate; M6: MET–*para*-hydroxybenzoic acid conjugate; M7: MET–coumaric acid conjugate; M8: MET–protocatechuic acid conjugate; M9: MET–salicylic acid conjugate; M10: MET–vanillic acid conjugate; temp.: Temperature.

molecular docking were performed using PyRx-AutoDock software (PyRx is open-source, user-friendly virtual screening software for computational drug discovery; https://pyrx.sourceforge.io/), and interactions within the docking complexes were analyzed using Discovery Studio Visualizer (Dassault Systèmes BIOVIA, France). Docking scores were interpreted such that more negative values indicated stronger binding affinities, as predicted by AutoDock (Scripps Research Institute, USA).[32]

2.2. Prediction of physicochemical properties and toxicity

Physicochemical criteria, known as Lipinski's Rule of Five (RO5), were applied to identify ideal oral drug candidates. RO5 defines standardized parameters based on chemical structure that predict oral bioavailability, facilitating the selection of optimal drug compounds.[30,33,34] The SwissADME tool was used to record the physicochemical profiles, including molecular weight (MW), the number of hydrogen bond acceptors and hydrogen bond donors, the partition coefficient between *n*-octanol and water (logP), and the topological surface area (http://www.swissadme.ch/). The ProTox tool (http://tox.charite.de/protoxII/) was used to predict toxicity profiles, including hepatotoxicity, carcinogenicity, immunotoxicity, mutagenicity, cytotoxicity, toxicity class, and the median lethal dose (LD_{50} in mg/kg), based on the chemical structures of individual native, hybrid, and standard drugs.[33]

2.3. Prediction of the absorption, distribution, metabolism, excretion, and toxicity properties and drug-likeness profiles

We assessed the absorption, distribution, metabolism, excretion, and toxicity profiles of the proposed hybrids and standard anti-cancer drugs using the SwissADME tool (SIB Swiss Institute of Bioinformatics, Switzerland). The tool predicted blood–brain barrier (BBB) penetration, gastrointestinal absorption, P-glycoprotein (P-gp) substrate status, interactions with cytochrome P450 enzymes, bioavailability scores, and skin permeability coefficients. In addition, the MolSoft tool (ICM-Pro, MolSoft LLC, USA) was used to predict drug-likeness scores and select lead candidates.[32,33]

Table 1. Anti-cancer potency, measured as molecular docking scores (kcal/mol), for selected phenolic acids (A1–A10) and their hybrid forms with MET (M1–M10) against two target enzymes, including their druggability profiles

S. No.	Molecular docking scores		Predicted druggability profiles					
	ALOX5 (PDB ID: 7TTL)	MMP9 (PDB ID: 1GKC)	RO5 (Y/N)	DLS	LLS	BA	LD_{50} (mg/kg)	TC
A1	−5.9	−6.3	Y	−1.00	No	0.85	290	III
A2	−6.5	−7.0	Y	−1.17	No	0.85	2,500	V
A3	−7.3	−7.7	Y	−0.35	No	0.56	2,980	V
A4	−7.0	−7.3	Y	−0.61	No	0.85	1,772	IV
A5	−6.6	−6.5	Y	−0.22	No	0.56	2,000	IV
A6	−6.2	−6.4	Y	−0.37	No	0.85	2,200	V
A7	−6.8	−7.2	Y	−0.81	No	0.85	2,850	V
A8	−6.5	−6.7	Y	0.23	No	0.56	2,000	IV
A9	−6.1	−7.1	Y	0.02	No	0.85	1,034	IV
A10	−6.6	−6.6	Y	−0.18	No	0.85	2,000	IV
M1	−8.3	−9.0	Y	−0.38	No	0.55	520	IV
M2	−8.2	−9.3	Y	0.06	Yes	0.55	600	IV
M3	−8.8	−9.6	Y	0.65	Yes	0.55	456	IV
M4	−7.7	−9.0	Y	0.16	No	0.55	640	IV
M5	−8.6	−9.4	Y	0.95	Yes	0.55	2,750	IV
M6	−8.5	−9.1	Y	0.70	No	0.55	2,000	IV
M7	−8.2	−9.1	Y	0.57	Yes	0.55	500	IV
M8	−8.4	−9.3	Y	0.96	Yes	0.55	2,750	IV
M9	−8.3	−9.2	Y	0.77	No	0.55	2,300	IV
M10	−7.6	−9.1	Y	0.44	Yes	0.55	1,950	IV
MET*	−5.5	−5.1	Y	−0.82	No	0.55	680	IV
DOX*	−9.1	−8.3	N	0.97	No	0.17	205	III
MT*	−6.3	−7.3	Y	−0.93	No	0.55	2,000	IV

Notes: *DOX and MT served as standard reference drugs for comparison with MET.

Abbreviations: ALOX5: Arachidonate 5-lipoxygenase; A1: Benzoic acid; A2: Cinnamic acid ; A3: Caffeic acid; A4: Ferulic acid; A5: Gallic acid; A6: *para*-hydroxybenzoic acid; A7: *para*-coumaric acid; A8: Protocatechuic acid; A9: Salicylic acid; A10: Vanillic acid; BA: Bioavailability; DLS: Drug-likeness score; DOX: Doxorubicin; LD50: Median lethal dose; LLS: Lead-likeness score; MET: Metformin; MMP9: Matrix metalloproteinase 9; MT: Marimastat; M1: MET–benzoic acid conjugate; M2: MET–cinnamic acid conjugate; M3: MET–caffeic acid conjugate; M4: MET–ferulic acid conjugate; M5: MET–gallic acid conjugate; M6: MET–*para*-hydroxybenzoic acid conjugate; M7: MET–coumaric acid conjugate; M8: MET–protocatechuic acid conjugate; M9: MET–salicylic acid conjugate; M10: MET–vanillic acid conjugate; N: No; PDB: Protein Data bank; RO5: Lipinski Rule of Five; TC: Toxic class; Y: Yes.

2.4. Molecular dynamics simulation

For 100-nanosecond molecular dynamics simulations, we chose four complexes—MMP9-A3, MMP9-M3, MMP9-MET, and MMP9-MT—based on docking scores and drug-likeness profiles. Protein-ligand interactions were simulated using the GROMACS 2022 program (https://www.gromacs.org/) and the AMBER99SB-ILDN force field to assess complex stability.[34,35] Following established procedures, the ACPYPE server was used to compute the ligand parameters and prepare the systems for molecular dynamics simulation.[32,35] Root-mean-square deviation (RMSD) and root-mean-square fluctuation (RMSF) plots were computed from the molecular dynamics trajectories using the "gmx rms" and "gmx rmsf" commands, respectively. In addition, the radius of gyration for each MMP9 system over the 100-nanosecond simulation period was analyzed using the "gmx gyrate" command.[32,35]

3. Results

3.1. Ligand readiness and receptor site choice for docking studies

We recorded the molecular docking scores of phenolic acids (A3–A10) and MET–phenolic acid conjugates (M1–M10), as well as MET and two standard drugs, DOX and MT, along with their binding affinity against the two target enzymes (ALOX5 and MMP9) (**Table 1**). Phenolic acids showed a range of docking scores against ALOX5 from –6 to –7 kcal/mol, but much greater binding affinity against MMP9, with scores ranging from –6 to –8 kcal/mol. A3 (caffeic acid) was the most active phenolic acid among the 10, exhibiting docking scores of –7.3 and –7.7 kcal/mol for the two target enzymes, respectively, whereas MET exhibited scores of –5.5 and –5.1 kcal/mol (**Table 1**). In addition, MET exhibited highly effective binding to both target enzymes when chemically hybridized with 10 distinct phenolic acids (M1–M10). The hybrid candidates demonstrated binding affinity against ALOX5, with docking scores ranging from –7 to –9 kcal/mol, while the scores against MMP9 were relatively higher, reaching up to –10 kcal/mol (**Table 1**). M3 (MET–A3) followed the same pattern as the individual phytochemicals, exhibiting relatively high binding affinities of –8.8 and –9.6 kcal/mol for the two target enzymes. When compared with the two United States Food and Drug Administration-approved anti-cancer drugs, DOX and MT, M3 exhibited a binding affinity equivalent to that of DOX (–9.1 and –8.3 kcal/mol). Nevertheless, MT, an MMP-9 inhibitor, exhibited weaker binding interactions (–6.3 and –7.3 kcal/mol) than the conjugated hybrids. From the perspective of protein–ligand interactions, M3 formed

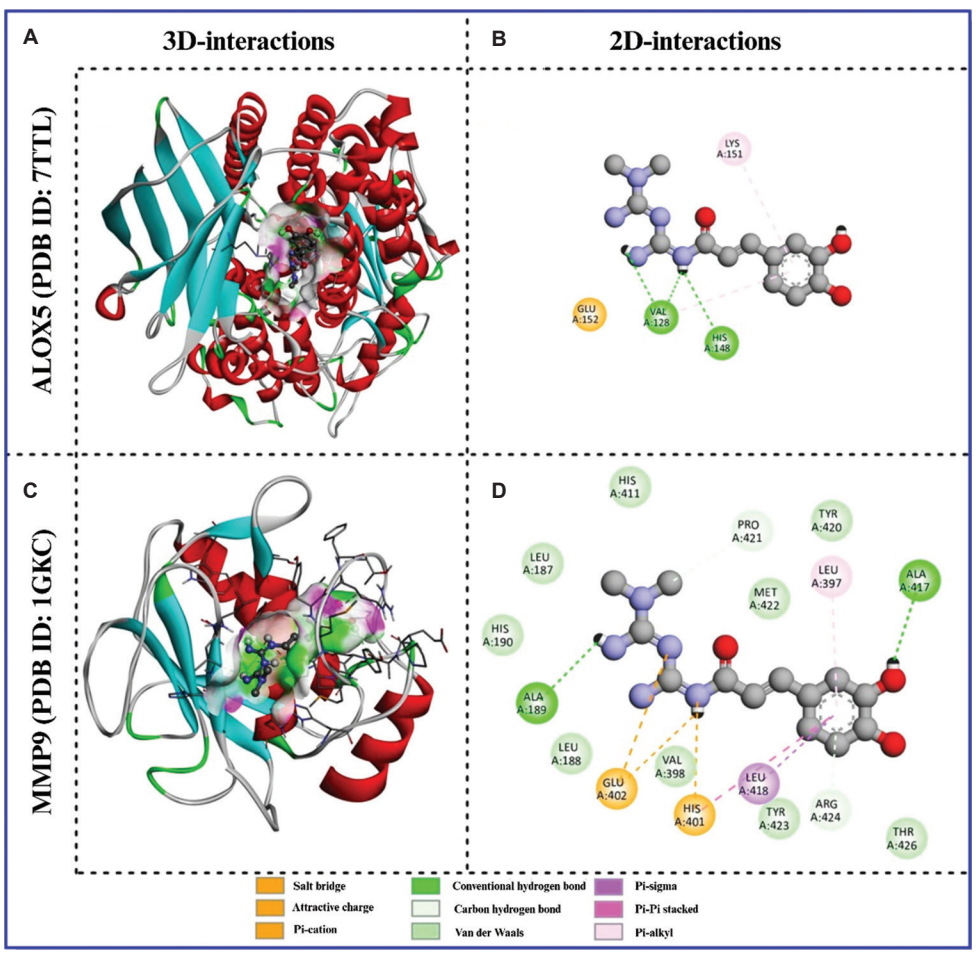

Figure 2. Protein–ligand interactions of the most promising hybrid candidate (M3: metformin–caffeic acid) against two putative target enzymes, visualized in 3D and 2D using Discovery Studio Visualizer (Dassault Systèmes BIOVIA, France)
Abbreviations: ALA: Alanine; ARG: Arginine; GLU: Glutamine; HIS: Histidine; LEU: Leucine; MET: Methionine; PRO: Proline; THR: Threonine: TYR: Tyrosine; VAL: Valine.

a greater number of noncovalent connections with MMP9 compared to ALOX5, suggesting that M3 exhibited superior binding affinity (**Figure 2**). Overall, docking scores indicated that the hybrid candidates were more effective than the individual compounds, suggesting that this strategy may be suitable for developing future anti-cancer drugs.

3.2. Assessment of physicochemical properties and potential toxicity

We analyzed the RO5 profiles for phenolic acids, conjugated hybrids, MET, MT, and DOX (**Table 2**). The recorded profiles indicated that all candidates, except DOX, met the ideal parameters of RO5, primarily because of their elevated MWs. This observation was consistent for the proposed hybrid candidates, which have the potential to serve as active oral drug candidates (**Tables 1** and **2**). Typically, a high XlogP score for a hybrid candidate suggests the potential to advance a lead compound into mainstream medicine. The RO5 information helped us identify the optimum oral candidates.

Tables 1 and **2** also present the LD_{50} and toxicity profiles. The predicted toxicity profiles show that phenolic acids are generally safer than the conjugated hybrids. [d]indicated that A4 had an elevated immunogenicity risk, whereas A3 and A8 exhibited a substantial carcinogenicity risk (**Table 2**). A5 and A7 had low carcinogenicity profiles, indicated by[c], whereas A1, A2, and A9 showed a moderate possibility of hepatotoxicity. M3, M4, M10, and DOX exhibited significant immunotoxicity risks, whereas the other profiles were classified as[b] and[a], indicating moderate and high safety, respectively. In terms of toxicity, phenolic acids and conjugated hybrids were classified in classes IV and V, respectively, suggesting that they may be toxic at higher doses (2,000–5,000 mg/kg). On the other hand, A3 and DOX were placed in lower categories, indicating that they may be toxic at lower concentrations (50–200 mg/kg) (**Table 1**). Overall, the toxicity profiles indicate that the hybrid candidates are safer than DOX.

3.3. Absorption, distribution, metabolism, excretion, and toxicity and drug-likeness profile prediction

Table 3 displays the pharmacokinetic characteristics of the phenolic acids, conjugated hybrids, and standard drugs. All potential candidates, except M5 and DOX, showed high

Table 2. Physicochemical profiles based on the Lipinski Rule of Five, along with predicted toxicity profiles of phenolic acids (A1–A10) and their hybrid forms with MET (M1–M10)

S. No.	Lipinski rule of five					Toxicity profiles				
	MW	XlogP	HBD	HBA	tPSA	HP	CG	IT	MG	CT
A1	122.12	1.87	1	2	37.30	A(0.54)[c]	IA(0.74)[a]	IA(0.99)[a]	IA(0.99)[a]	IA(0.86)[a]
A2	148.16	2.13	1	2	37.30	A(0.54)[c]	IA(0.82)[a]	IA(0.95)[a]	IA(0.96)[a]	IA(0.83)[a]
A3	180.16	1.15	3	4	77.76	IA(0.57)[b]	A(0.78)[d]	IA(0.50)[b]	IA(0.98)[a]	IA(0.86)[a]
A4	194.18	1.51	2	4	66.76	IA(0.51)[b]	IA(0.61)[b]	A(0.91)[d]	IA(0.96)[a]	IA(0.88)[a]
A5	170.12	0.70	4	5	97.99	IA(0.61)[b]	A(0.56)[c]	IA(0.99)[a]	IA(0.94)[a]	IA(0.91)[a]
A6	138.12	1.58	2	3	57.53	IA(0.52)[b]	IA(0.51)[b]	IA(0.99)[a]	IA(0.99)[a]	IA(0.86)[a]
A7	164.16	1.46	2	3	57.53	IA(0.51)[b]	A(0.50)[c]	IA(0.91)[a]	IA(0.93)[a]	IA(0.81)[a]
A8	154.12	1.15	3	4	77.76	IA(0.59)[b]	A(0.72)[d]	IA(0.99)[a]	IA(0.97)[a]	IA(0.90)[a]
A9	138.12	2.26	2	3	57.53	A(0.51)[c]	IA(0.67)[b]	IA(0.99)[a]	IA(0.98)[a]	IA(0.86)[a]
A10	168.15	1.43	2	4	66.76	IA(0.55)[b]	IA(0.64)[b]	IA(0.97)[a]	IA(0.96)[a]	IA(0.93)[a]
M1	233.27	1.33	4	3	92.07	IA(0.62)[b]	IA(0.67)[b]	IA(0.98)[a]	IA(0.70)[a]	IA(0.68)[b]
M2	259.31	1.76	4	3	92.07	IA(0.60)[b]	IA(0.64)[b]	IA(0.81)[a]	IA(0.70)[a]	IA(0.67)[b]
M3	291.31	1.03	6	5	132.53	IA(0.59)[b]	IA(0.57)[b]	A(0.86)[d]	IA(0.65)[b]	IA(0.60)[b]
M4	305.33	1.39	5	5	121.53	IA(0.58)[b]	IA(0.59)[b]	A(0.98)[d]	IA(0.64)[b]	IA(0.69)[b]
M5	281.27	0.82	7	6	152.76	IA(0.62)[b]	IA(0.56)[b]	IA(0.75)[a]	IA(0.66)[b]	IA(0.69)[b]
M6	249.27	0.98	5	4	112.30	IA(0.61)[b]	IA(0.59)[b]	IA(0.95)[a]	IA(0.69)[b]	IA(0.70)[a]
M7	275.31	1.40	5	4	112.30	IA(0.59)[b]	IA(0.58)[b]	IA(0.62)[b]	IA(0.69)[b]	IA(0.70)[a]
M8	265.27	1.03	6	5	132.53	IA(0.62)[b]	IA(0.57)[b]	IA(0.77)[a]	IA(0.66)[b]	IA(0.67)[b]
M9	249.27	0.07	5	4	112.30	IA(0.62)[b]	IA(0.59)[b]	IA(0.76)[a]	IA(0.65)[b]	IA(0.70)[a]
M10	279.30	1.31	5	5	121.53	IA(0.60)[b]	IA(0.59)[b]	A(0.79)[d]	IA(0.65)[b]	IA(0.69)[b]
MET	129.16	−1.3	3	1	91.5	IA(0.74)[a]	IA(0.68)[b]	IA(0.99)[a]	IA(0.59)[b]	IA(0.69)[b]
DOX	543.5	1.3	6	12	206	IA(0.86)[a]	IA(0.90)[a]	A(0.99)[d]	A(0.98)[d]	A(0.94)[d]
MT	331.41	0.5	5	5	128	IA(0.56)[b]	IA(0.54)[b]	IA(0.97)[a]	IA(0.54)[b]	IA(0.59)[b]

Note: The letters "A" and "IA" denote active and inactive profiles, respectively, with [a]indicating safe, [b]moderately safe, [c]moderate risk, and [d]high risk.
Abbreviations: A1: Benzoic acid; A2: Cinnamic acid; A3: Caffeic acid; A4: Ferulic acid; A5: Gallic acid; A6: *para*-hydroxybenzoic acid; A7: *para*-coumaric acid; A8: Protocatechuic acid; A9: Salicylic acid; A10: Vanillic acid; CG: Carcinogenicity; CT: Cytotoxicity; DOX: Doxorubicin; HBA: Hydrogen bond acceptor; HBD: Hydrogen bond donor; HP: Hepatotoxicity; IT: Immunotoxicity; MET: Metformin; MG: Mutagenicity; MT: Marimastat; MW: Molecular weight; M1: MET–benzoic acid conjugate; M2: MET–cinnamic acid conjugate; M3: MET–caffeic acid conjugate; M4: MET–ferulic acid conjugate; M5: MET–gallic acid conjugate; M6: MET–*para*-hydroxybenzoic acid conjugate; M7: MET–coumaric acid conjugate; M8: MET–protocatechuic acid conjugate; M9: MET–salicylic acid conjugate; M10: MET–vanillic acid conjugate; tPSA: Topological polar surface area; XlogP: Partition coefficient between *n*-octanol and water.

Table 3. Predicted pharmacokinetic profiles of phenolic acids (A1 to A10) and their hybrid forms with MET (M1–M10)

S. No.	GI_{abs}	BBB	P-gp	CYP1A2	CYP2C19	CYP2C9	CYP2D6	CYP3A4	Log Kp
A1	High	Yes	No	No	No	No	No	No	−5.72
A2	High	Yes	No	No	No	No	No	No	−5.69
A3	High	No	No	No	No	No	No	No	−6.58
A4	High	Yes	No	No	No	No	No	No	−6.41
A5	High	No	No	No	No	No	No	Yes	−6.84
A6	High	Yes	No	No	No	No	No	No	−6.02
A7	High	Yes	No	No	No	No	No	No	−6.26
A8	High	No	No	No	No	No	No	Yes	−6.42
A9	High	Yes	No	No	No	No	No	No	−5.54
A10	High	No	No	No	No	No	No	No	−6.31
M1	High	No	No	No	No	No	No	No	−6.78
M2	High	No	No	No	No	No	No	No	−6.63
M3	High	No	No	No	No	No	No	No	−7.35
M4	High	No	No	No	No	No	No	No	−7.18
M5	Low	No	No	No	No	No	No	No	−7.43
M6	High	No	No	No	No	No	No	No	−7.12
M7	High	No	No	No	No	No	No	No	−6.99
M8	High	No	No	No	No	No	No	No	−7.19
M9	High	No	No	No	No	No	No	No	−7.77
M10	High	No	No	No	No	No	No	No	−7.07
MET	High	No	No	No	No	No	No	No	−7.99
DOX	Low	No	Yes	No	No	No	No	No	−8.71
MT	High	No	No	No	No	No	No	No	−7.96

Abbreviations: A1:. Benzoic acid; A2: Cinnamic acid ; A3: Caffeic acid; A4: Ferulic acid; A5: Gallic acid; A6: *para*-hydroxybenzoic acid; A7: *para*-coumaric acid; A8: Protocatechuic acid; A9: Salicylic acid; A10: Vanillic acid; BBB: Blood–brain barrier; DOX: Doxorubicin; GI_{abs}: Gastrointestinal absorption; Log Kp: Skin permeability coefficients; MET: Metformin; MT: Marimastat; M1: MET–benzoic acid conjugate; M2: MET–cinnamic acid conjugate; M3: MET–caffeic acid conjugate; M4: MET–ferulic acid conjugate; M5: MET–gallic acid conjugate; M6: MET–*para*-hydroxybenzoic acid conjugate; M7: MET–coumaric acid conjugate; M8: MET–protocatechuic acid conjugate; M9: MET–salicylic acid conjugate; M10: MET–vanillic acid conjugate; P-gp: p-glycoprotein.

gastrointestinal absorption according to the data. However, A1, A2, A4, A6, A7, and A9 demonstrated the ability to cross the BBB. Another desirable pharmacokinetic property of the conjugated hybrids is that they do not cross the BBB, in contrast to some hybrid candidates that show a tendency similar to the standard drugs. In addition, P-gp transporter interactions, as well as the skin permeability coefficient profiles, indicated that when phenolic acids are chemically combined with MET, they exhibit improved pharmacokinetic profiles compared to pure phenolic acids (**Table 3**). Drug-likeness scores were favorable for the conjugated hybrid candidates but unfavorable for the individual phenolic acids. While most hybrids exhibited a lead-likeness score and a higher probability of clinical success, the phenolic acids did not possess lead-likeness scores. However, MET and MT demonstrated negative drug-likeness scores. In **Figure 3**, we present a comparative analysis of phenolic acid A3, the conjugated hybrid M3, conventional MET, and MT profiles. Chemical conjugation with MET appeared to be a promising strategy for developing new anti-cancer drugs by leveraging the most effective phenolic acids and enhancing drug-likeness profiles for practical applications.

3.4. Molecular dynamics simulation

We analyzed the stability and dynamics of the MMP9–A3, MMP9–MET, MMP9–M3, and MMP9–MT docking complexes over a 100-nanosecond time frame. **Figure 4** presents the molecular docking parameters.

Root-mean-square deviation analysis revealed that all complexes underwent an initial equilibration phase with deviations during the first 1–25 nanoseconds, followed by a stable phase between 26 and 60 nanoseconds, and moderate fluctuations toward the end of the trajectory (**Figure 4A**). Among them, MMP9–M3 showed the lowest overall deviation (0.2–0.3 nm), indicating higher structural stability, whereas MMP9–MET and MMP9–MT exhibited larger fluctuations (0.1–0.4 nm). Ligand RMSD profiles further confirmed that while all ligands deviated during the first 25 nanoseconds, M3 and A3 subsequently attained highly stable conformations. In contrast, MT remained comparatively unstable until the end of the simulation (**Figure 4B**).

Root-mean-square fluctuation plots demonstrated residue-level flexibility, with all complexes showing pronounced fluctuations within the 170–200 residue region. Notably, MMP9–M3 exhibited an additional deviation around residue 410 extending to the C-terminal region, possibly reflecting adaptive binding dynamics (**Figure 4C**).

Radius of gyration analysis revealed the compactness of protein structures across all complexes, with similar fluctuations observed up to 20 nanoseconds. MMP9–M3 maintained a more consistent radius of gyration profile beyond this period

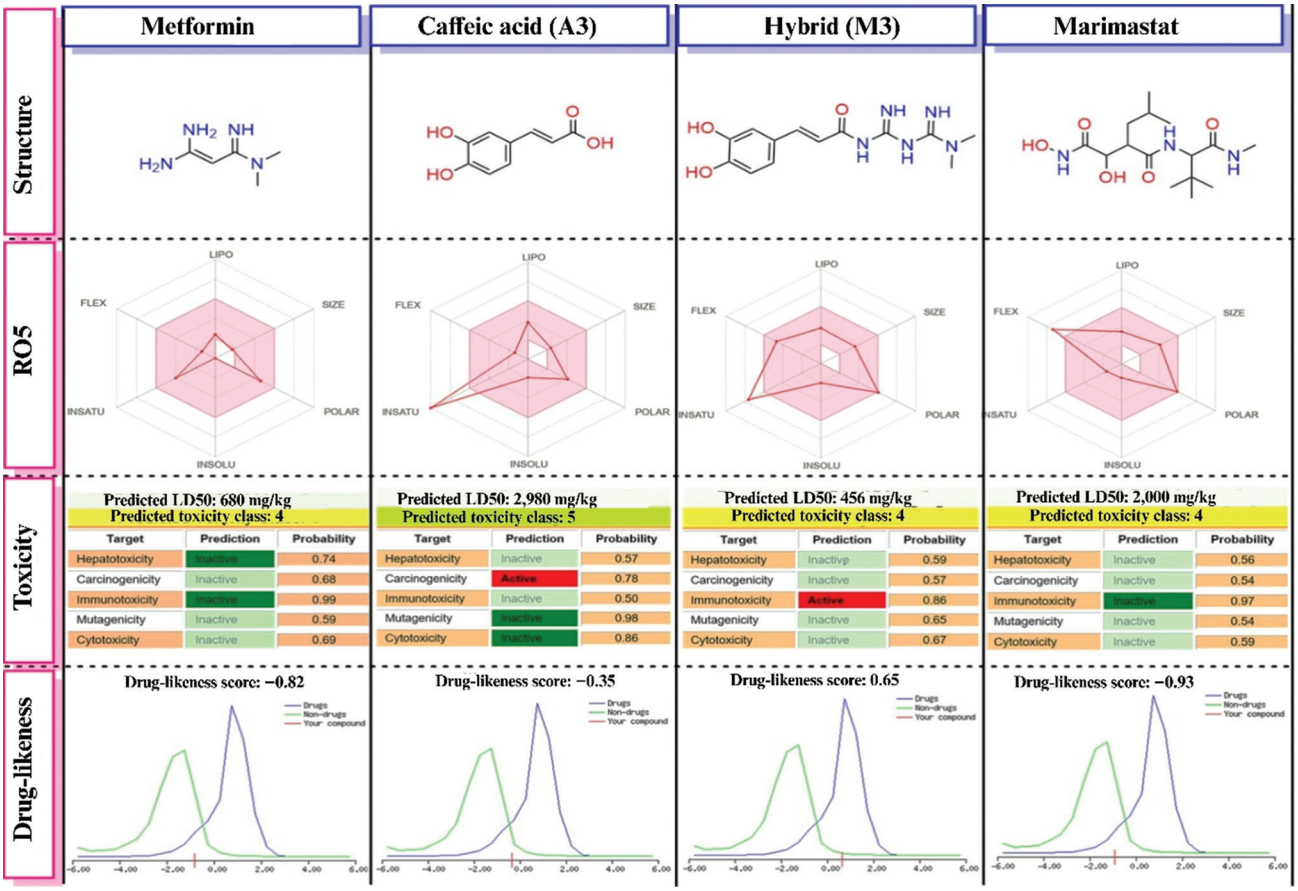

Figure 3. Graphical illustration of chemical structures with respect to predicted physicochemical profiles (Lipinski RO5), toxicity profiles, and overall drug-likeness scores of metformin, caffeic acid, and their proposed hybrid form (M3), along with an MMP9 inhibitor standard anti-cancer drug in a comparative analysis platform

Abbreviations: Flex: Flexibility; Insatu: Unsaturation; Insolu: Insolubility; LD_{50}: Median lethal dose; Lipo: Lipophilicity; MMP9: Matrix metalloproteinase 9; M3: Metformin–caffeic acid conjugate; RO5: Rule of five.

compared with other complexes, suggesting a more stable and compact structure overall (**Figure 4D**).

Hydrogen bond analysis further supported these observations. MMP9–M3 maintained a higher and more consistent number of hydrogen bonds (7–8 throughout the trajectory; **Figure 4F**), compared to A3 (initially 5, dropping to 2; **Figure 4E**), MT (5 decreasing to 2; **Figure 4G**), and MET (constant at ~6; **Figure 4H**).

Taken together, the molecular dynamics results illustrate that the MMP9–M3 complex exhibits superior dynamic stability, compactness, and persistent hydrogen bonding compared with the other tested complexes, supporting its potential as a promising candidate for targeting MMP9 in cancer therapy.

4. Discussion

Continued research into phytochemical hybridization promises to revolutionize cancer treatment by improving patient outcomes through diverse and complex anti-cancer mechanisms.[16,17,35] These compounds regulate intracellular signaling pathways that control the cell cycle, DNA repair, and apoptosis, while also inhibiting angiogenesis and metastasis.[18,19,25] Although phytochemicals show promising therapeutic potential, challenges, such as poor bioavailability, complex mechanisms, and the need for clinical translation hinder their development as anti-cancer agents.

Based on computational analyses, we examined the structure–activity relationships of individual and native candidates, demonstrating that MET conjugated with cinnamic acid (M3) exhibits superior anti-cancer efficacy and drug-likeness compared to MET–benzoic acid hybrids. MET and A3 individually exhibited potential anti-cancer effects; however, their chemical conjugation produced a lead candidate (M3) with enhanced efficacy. The position of the hydroxyl group in benzoic and cinnamic acids significantly modulates their biological potency.

While many studies of this nature already exist,[21,24,25] this investigation stands out by employing an advanced computer-aided drug design platform that systematically identifies potential leads before experimental evaluation. By narrowing the field down to the most promising candidate with the highest likelihood of clinical success, this approach may ultimately save time and resources in the drug development process. Utilizing a synergistic medicinal chemistry approach that combines known drugs with bioactive phytochemicals or scaffolds offers a promising solution to circumvent challenges associated with drug unavailability and to facilitate the development of effective novel agents.

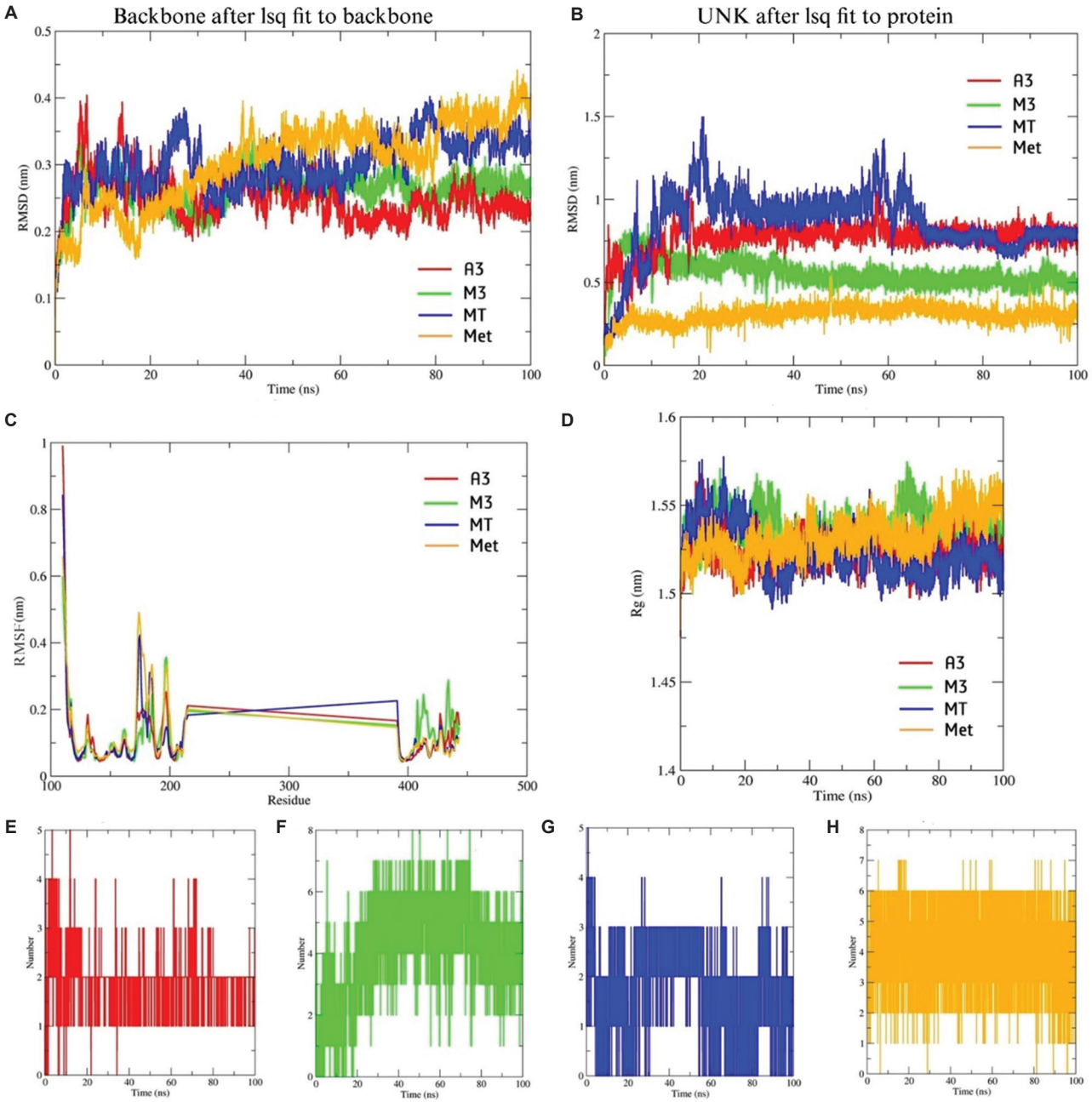

Figure 4. Molecular dynamics simulations demonstrating the conformational stability of caffeic acid (A3), metformin–caffeic acid conjugate (M3), and metformin (MET), compared with the standard drug marimastat (MT), complexed with the target enzyme matrix metalloproteinase 9 (MMP9) over 100 nanoseconds. (A) Root-mean-square deviation (RMSD) plots of backbone proteins; (B) RMSD plots of ligands; (C) Root-mean-square fluctuation (RMSF) plots; (D) Radius of gyration (Rg) plots; (E), Hydrogen bond interactions of A3; (F) Hydrogen bond interactions of M3; (G) Hydrogen bond interactions of MT; and (H) Hydrogen bond interactions of MET.
Abbreviations: lsq: Least squares; UNK: Unknown ligand.

Academic and pharmaceutical researchers often employ computational or bioinformatics methods during the early phases of drug development to gather additional information on the druggability of rejected candidates and to advance promising candidates into further experimental trials.[33-36] Coding and programming form the backbone of computational tools, allowing researchers to narrow down the field to a manageable number of candidates for validation through rigorous cross-verification in both *in vitro* and *in vivo* models. This process ensures reproducibility, enhances experimental robustness, and confirms the reliability of findings before mainstream application. In addition, to obtain more accurate findings and greater experimental success, it is essential to have a well-formulated hypothesis and a basic understanding of coding or programming.[35-38] The phytochemical-based approach provides an effective strategy for repurposing existing drugs and platforms, facilitating the integration of bioactive phytochemicals into mainstream therapeutic applications.

5. Conclusions

Present circumstances demand the development of novel therapeutic candidates to reduce cancer mortality and improve patient survival rates. MET–phenolic acid conjugates, particularly those involving cinnamic acid, have been identified as potent candidates in innovative oncology drug discovery. To maximize the therapeutic efficacy of these compounds in oncology, it is essential to conduct thorough research to delineate their mode of action, refine their pharmacological profiles, and systematically evaluate their clinical effectiveness. The combined application of molecular docking and molecular dynamics simulations has facilitated the rational design and optimization of MET–phenolic acid hybrids with enhanced anti-cancer efficacy. The transformation of anti-diabetic drugs into anti-cancer agents through conjugation with phenolic acids represents a highly effective strategy for combating cancer. Phenolic acids demonstrated anti-cancer activity only at higher concentrations and exhibited limited druggability, limiting their widespread therapeutic use. Chemical hybridization with MET–caffeic acid (M3) resulted in improved docking scores, enhanced stability, and favorable druggability profiles. Further experimental validation is required to confirm its anti-cancer potential and to substantiate computational findings for clinical application. In this study, we demonstrated that the M3 hybrid exhibited superior stability, drug-likeness, and predicted safety compared to other hybrids and reference compounds. These findings are consistent with previous reports on the anti-cancer activities of MET and caffeic acid, supporting the potential of hybrid molecules as promising candidates. In addition to the promising *in silico* outcomes, it is essential to acknowledge that our study lacks direct experimental validation of the interaction between M3 (caffeic acid and MET) and its target proteins. Future studies will therefore focus on employing molecular biology techniques, such as western blotting to assess changes in pathway-related protein expression, and surface plasmon resonance to quantify kinetic interaction profiles. These approaches will be crucial for confirming the predicted interactions, strengthening the mechanistic understanding of M3, and bridging the gap between computational predictions and biological validation. Such follow-up studies could establish the mechanism of action of M3 in cancer models and evaluate its therapeutic potential *in vivo*.

Acknowledgement
The authors are grateful to the President of Siksha 'O' Anusandhan, Bhubaneswar, Odisha, India, for his support in facilitating the research work and providing the necessary resources.
Financial support
This study was funded by Siksha 'O' Anusandhan, Bhubaneswar, Odisha, India, through the doctoral fellowship awarded to Mr. Biswajit Banerjee (Ref. No. (Acad) Regr/4266/SOADU).
Conflicts of interest statement
The authors declare no conflicts of interest.
Author contributions
Conceptualization: BB, TS, and AM; *Formal analysis*: AM; *Methodology*: BB; *Supervision*: TS and AM; *Visualization*: BB, TS, and AM; *Writing – original draft*: BB and AM; *Writing – review & editing:* AM. All authors have read and agreed to the published version of the manuscript.
Ethics approval and consent to participate
Not applicable.
Consent for publication
Not applicable.
Availability of data
All original data presented in this study are included in the article.

References

1. *WHO-Global Cancer Observatory-2024.* Available from: https://gco.iarc.fr/en [Last accessed on 2025 May 20].
2. Siegel RL, Miller KD, Wagle NS, Jemal A. Cancer statistics, 2023. *CA Cancer J Clin.* 2023;73(1):17-48. doi: 10.3322/caac.21763
3. Yang Q, Xu D, Yang Y, Lu S, Wang D, Wang L. Global, regional, and national burden of gastric cancer in adolescents and young adults, 1990-2019: A systematic analysis for the global burden of disease study 2019. *Am J Gastroenterol.* 2024;119(3):454-467. doi: 10.14309/ajg.0000000000002551
4. Garner WB, Smith BD, Ludmir EB, *et al.* Predicting future cancer incidence by age, race, ethnicity, and sex. *J Geriatr Oncol.* 2023;14(1):101393. doi: 10.1016/j.jgo.2022.10.008
5. Elmore LW, Greer SF, Daniels EC, *et al.* Blueprint for cancer research: Critical gaps and opportunities. *CA Cancer J Clin.* 2021;71(2):107-139. doi: 10.3322/caac.21652
6. Jacquemin V, Antoine M, Dom G, Detours V, Maenhaut C, Dumont JE. Dynamic cancer cell heterogeneity: Diagnostic and therapeutic implications. *Cancers (Basel).* 2022;14(2):280. doi: 10.3390/cancers14020280
7. Fares J, Fares MY, Khachfe HH, Salhab HA, Fares Y. Molecular principles of metastasis: A hallmark of cancer revisited. *Signal Transduct Target Ther.* 2020;5(1):28. doi: 10.1038/s41392-020-0134-x
8. Zhong L, Li Y, Xiong L, *et al.* Small molecules in targeted cancer therapy: Advances, challenges, and future perspectives. *Signal Transduct Target Ther.* 2021;6(1):201. doi: 10.1038/s41392-021-00572-w
9. Naeem A, Hu P, Yang M, *et al.* Natural products as anti cancer agents: Current status and future perspectives. *Molecules.* 2022;27(23):8367. doi: 10.3390/molecules27238367
10. Huang M, Lu JJ, Ding J. Natural products in cancer therapy: Past, present and future. *Nat Prod Bioprospect.* 2021;11(1):5-13. doi: 10.1007/s13659-020-00293-7
11. Grover P, Thakur K, Bhardwaj M, Mehta L, Raina SN, Rajpal VR. Phytotherapeutics in cancer: From potential drug candidates to clinical translation. *Curr Top Med Chem.* 2024;24:1050-1074. doi: 10.2174/0115680266282518231231075311
12. Anantharaju PG, Gowda PC, Vimalambike MG, Madhunapantula SV. An overview on the role of dietary phenolics for the treatment of cancers. *Nutr J.* 2016;15(1):99. doi: 10.1186/s12937-016-0217-2
13. Kumar N, Goel N. Phenolic acids: Natural versatile molecules with promising therapeutic applications. *Biotechnol Rep (Amst).* 2019;24:e00370. doi: 10.1016/j.btre.2019.e00370
14. Abotaleb M, Liskova A, Kubatka P, Büsselberg D. Therapeutic potential of plant phenolic acids in the treatment of cancer. *Biomolecules.* 2020;10(2):221. doi: 10.3390/biom10020221
15. Stielow M, Witczyńska A, Kubryń N, Fijałkowski Ł, Nowaczyk J, Nowaczyk A. The bioavailability of drugs: The current state of knowledge. *Molecules.* 2023;28(24):8038. doi: 10.3390/molecules28248038
16. Swain SS, Paidesetty SK, Padhy RN, Hussain T. Isoniazid-phytochemical conjugation: A new approach for potent and less toxic anti-TB drug development. *Chem Biol Drug Des.* 2020;96(2):714-730. doi: 10.1111/cbdd.13685

17. Micale N, Molonia MS, Citarella A, *et al.* Natural product-based hybrids as potential candidates for the treatment of cancer: Focus on curcumin and resveratrol. *Molecules.* 2021;26(15):4665. doi: 10.3390/molecules26154665
18. Sflakidou E, Leonidis G, Foroglou E, Siokatas C, Sarli V. Recent advances in natural product-based hybrids as anti-cancer agents. *Molecules.* 2022;27(19):6632. doi: 10.3390/molecules27196632
19. Swain SS, Sahoo A, Singh SR, Sahoo J, Paidesetty SK. Synthesis, spectroscopic analysis, and computational-based investigations on 'azo-coumarin-Co(II)-galangin' hybrids exhibit multipotential activities. *J Biomol Struct Dyn.* 2024;43:7336-7347. doi: 10.1080/07391102.2024.2326666
20. Nankar R, Prabhakar PK, Doble M. Hybrid drug combination: Combination of ferulic acid and metformin as anti-diabetic therapy. *Phytomedicine.* 2017;37:10-13. doi: 10.1016/j.phymed.2017.10.015
21. Markowicz-Piasecka M, Huttunen KM, Broncel M, Sikora J. Sulfenamide and sulfonamide derivatives of metformin - A new option to improve endothelial function and plasma haemostasis. *Sci Rep.* 2019;9(1):6573. doi: 10.1038/s41598-019-43083-z
22. Masadeh MM, Alzoubi KH, Masadeh MM, Aburashed ZO. Metformin as a potential adjuvant antimicrobial agent against multidrug-resistant bacteria. *Clin Pharmacol.* 2021;13:83-90. doi: 10.2147/CPAA.S297903
23. Podhorecka M, Ibanez B, Dmoszyńska A. Metformin - its potential anti-cancer and anti-aging effects. *Postepy Hig Med Dosw (Online).* 2017;71(0):170-175. doi: 10.5604/01.3001.0010.3801
24. Jiang T, Chen L, Huang Y, *et al.* Metformin and docosahexaenoic acid hybrid micelles for premetastatic niche modulation and tumour metastasis suppression. *Nano Lett.* 2019;19(6):3548-3562. doi: 10.1021/acs.nanolett.9b00495
25. Bashraheel SS, Kheraldine H, Khalaf S, Moustafa AA. Metformin and HER2-positive breast cancer: Mechanisms and therapeutic implications. *Biomed Pharmacother.* 2023;162:114676. doi: 10.1016/j.biopha.2023.114676
26. Gong L, Goswami S, Giacomini KM, Altman RB, Klein TE. Metformin pathways: Pharmacokinetics and pharmacodynamics. *Pharmacogenet Genomics.* 2012;22(11):820-827. doi: 10.1097/FPC.0b013e3283559b22
27. Rusanov DA, Zou J, Babak MV. Biological properties of transition metal complexes with metformin and its analogues. *Pharmaceuticals (Basel).* 2022;15(4):453. doi: 10.3390/ph15040453
28. Banerjee B, Sharma T, Banerjee S, Banerjee S, Mondal A. Synthesis and anticancer activity of metforminphenolic acid conjugates. *Chem Biodivers.* 2025;22(6):e202403199. doi: 10.1002/cbdv.202403199
29. Oyedemi SO, Eze K, Aiyegoro OA, *et al.* Computational, chemical profiling and biochemical evaluation of antidiabetic potential of *Parkia biglobosa* stem bark extract in type 2 model of rats. *J Biomol Struct Dyn.* 2022;40(20):9948-9961. doi: 10.1080/07391102.2021.1938228
30. Sahoo A, Fuloria S, Swain SS, *et al.* Potential of marine terpenoids against SARS-CoV-2: An *in-silico* drug development approach. *Biomedicines.* 2021;9(11):1505. doi: 10.3390/biomedicines9111505
31. Ramorobi LM, Matowane GR, Mashele SS, *et al.* Bioactive synergism between zinc mineral and p-coumaric acid: A multi-mode glycemic control and antioxidative study. *J Food Biochem.* 2022;46(10):e14360. doi: 10.1111/jfbc.14360
32. Swain SS, Singh SR, Sahoo A, Panda PK, Hussain T, Pati S. Integrated bioinformatics-cheminformatics approach toward locating pseudo-potential antiviral marine alkaloids against SARS-CoV-2-Mpro. *Proteins.* 2022a;90(9):1617-1633. doi: 10.1002/prot.26341
33. Sahoo A, Swain SS, Paital B, Panda M. Combinatorial approach of vitamin C derivative and anti-HIV drug-darunavir against SARS-CoV-2. *Front Biosci (Landmark Ed).* 2022;27(1):10. doi: 10.31083/j.fbl2701010
34. Swain SS, Pati S, Hussain T. Quinoline heterocyclic containing plant and marine candidates against drug-resistant *Mycobacterium tuberculosis*: A systematic drug-ability investigation. *Eur J Med Chem.* 2022;232:114173. doi: 10.1016/j.ejmech.2022.114173
35. Mudedla SK, Braka A, Wu S. Quantum-based machine learning and AI models to generate force field parameters for drug-like small molecules. *Front Mol Biosci.* 2022;9:1002535. doi: 10.3389/fmolb.2022.1002535
36. Sadybekov AV, Katritch V. Computational approaches streamlining drug discovery. *Nature.* 2023;616(7958):673-685. doi: 10.1038/s41586-023-05905-z
37. Zhong F, Xing J, Li X, *et al.* Artificial intelligence in drug design. *Sci China Life Sci.* 2018;61(10):1191-1204. doi: 10.1007/s11427-018-9342-2
38. Jiménez-Luna J, Grisoni F, Weskamp N, Schneider G. Artificial intelligence in drug discovery: Recent advances and future perspectives. *Expert Opin Drug Discov.* 2021;16(9):949-959. doi: 10.1080/17460441.2021.1909567

Received: May 21, 2025
Revised: October 16, 2025
Accepted: October 17, 2025
Available online: December 19, 2025